A MODEL OF THE ENERGY TRANSFER IN STELLAR INTERIORS

We present a model of the convective and radiative layers in stellar interiors. With the energy transport model we presented in our previous paper (N/A 2023), we construct a new model of integrating our way from the stellar surface to the core. We are able to produce a model of a star with scaled solar parameters as initial values, which have a core reaching out to 15.29% of R_0, consisting of both a radiative layer and a convection layer. The star also has a convection zone near the surface, with a width of 14.42% of R_0.

I. INTRODUCTION

Observations of the Sun have been an important way of understanding how the stars in the vast universe work. In particular, solar sunspots were the main topic of discussion in the 16th and 17th centuries. The letter exchange between the Italian physicist and astronomer Galileo Galilei, and the Jesuit mathematician Christoph Scheiner in the early years of the 17th century still resonates today (The British Library 2023). Since then, mankind's knowledge about the solar interior has grown a lot. From Bethe's paper on nuclear fusion (Bethe 1939) to the Borexino collaboration's work on solar neutrinos The Borexino Collaboration (2018), our natural interest in the life-giving sphere 150 million kilometers away has only grown.

In this paper, we model a star numerically by integrating our way from the surface to the core. We take advantage of the results we presented in our previous paper (N/A 2023) and try to fit a model that reaches the goals described in Sect. II C 1. We aim towards modeling the different energy transfer layers of the star, namely the radiation zones and convection zones. In (N/A 2023), we presented the proton-proton (PP) chains and the carbon-nitrogen-oxygen (CNO) cycle, which are the only two ways of fusing hydrogen to helium (Gudiksen 2022).

The equations we use are presented and described in Sect. II, together with our molecular composition and numerical recipe. We present our results in Sect. III, where the figures and tables describe in detail how the model works. Before reaching our conclusion and describing how working with this model has been in Sect. V, we discuss all of our results in Sect. IV.

In Appendix A, we include the calculations of the temperature gradients used to compute the energy fluxes.

II. METHOD

A. Governing equations

The equations we use in this paper are as follows.

$$\frac{\partial r}{\partial m} = \frac{1}{4\pi r^2 \rho} \tag{1}$$

$$\frac{\partial P}{\partial m} = -\frac{Gm}{4\pi r^4} \tag{2}$$

$$\frac{\partial L}{\partial m} = \epsilon \tag{3}$$

$$\frac{\partial T}{\partial m} = \nabla \frac{T}{P} \frac{\partial P}{\partial m} \tag{4}$$

$$P_{\text{tot}} = P_{\text{rad}} + P_{\text{gas}} \tag{5}$$

1. *Radius*

We use m as the free variable, as the equations are more stable than if r is used. Eq. 1 represents how the radius changes as the mass changes. The symbols are the radius r in m, and the density within that radius, ρ in m^{-3}.

2. *Pressure*

Since we are assuming ideal gas, the ideal gas law is considered, commonly written as $PV = Nk_BT$, where $k_B = 1.381 \cdot 10^{-23}\,\text{JK}^{-1}$ is the Boltzmann constant. In this paper, we use the modified ideal gas law:

$$P = \frac{\rho}{\mu m_u} k_B T \tag{6}$$

Here, $n = \rho/(\mu m_u)$ is the number density, μ is the mean molecular weight, and $m_u = 1.661 \cdot 10^{-27}$ kg is the atomic mass constant. We have also used that $V = \rho^{-1}$, and that $N = n/V$. The star also has a radiative pressure, described by

$$P_{\text{rad}} = \frac{4\sigma T^4}{3c}, \tag{7}$$

where $\sigma = 5.670 \cdot 10^{-8}\,\text{Wm}^{-2}\text{K}^{-4}$ is the Stefan-Boltzmann constant, and $c = 2.998 \cdot 10^8\,\text{ms}^{-1}$ is the speed of light in vacuum. Eq. 6 becomes the function $P_{\text{gas}}(\rho, T)$. From Eq. 5, we find the expression

$$\rho(P_{\text{tot}}, T) = \Big(P_{\text{tot}} - P_{\text{rad}}\Big) \frac{\mu m_u}{k_B T} \tag{8}$$

The change in pressure due to a change in mass is described by Eq. 2, where $G = 6.674 \cdot 10^{-11}\,\mathrm{m^{-3}kg^{-1}s^{-2}}$ is the Newtonian constant of gravitation, and m is the mass in kg.

3. *Luminosity*

The total energy production is computed as the sum of the PP chains and the CNO cycle. In our previous paper (N/A 2023), we presented the model for calculating the energy released by these reactions. As luminosity is the measure of total electromagnetic power released per second, Eq. 3 shows that the change in luminosity equals the energy produced at the next step[1].

4. *Temperature*

The change in energy described in Eq. 4, is dependent on whether the gas inside the star is convectively stable or not, where

$$\nabla \equiv -\frac{H_P}{T}\frac{\partial T}{\partial r}, \tag{9}$$

and H_P is the pressure scale. The energy produced from the nuclear reactions is transported towards the surface in two ways (Gudiksen 2022). When photons are emitted, absorbed, and re-emitted, and the number of photons traveling outwards is slightly larger than photons traveling inwards, we have radiative transport of energy. The change in temperature (and Eq. 4) then becomes

$$\frac{\partial T}{\partial m} = -\frac{3\kappa L}{256\pi^2\sigma r^4 T^3}, \tag{10}$$

where κ is the opacity of the gas in $\mathrm{m^2g^{-1}}$, and L is the luminosity in $\mathrm{Js^{-1}}$. If the gas is convectively unstable, the gas begins to move, and the energy is transported by convection. The ∇ in Eq. 4 becomes ∇^* in Eq. A17. The convective instability criterion is $\nabla > \nabla_{\mathrm{ad}}$, where ∇_{ad} is the adiabatic temperature gradient. As we assume an ideal gas, it can be shown that

$$\nabla_{\mathrm{ad}} = \frac{2}{5}. \tag{11}$$

If there is no convection, the radiative flux F_{rad} is equal to the total flux, meaning

$$F_{\mathrm{rad}} = \frac{L}{4\pi r^2}, \tag{12}$$

and from Eq. A3, with F_{con} equal to zero, we get the stable temperature gradient

$$\nabla_{\mathrm{stable}} = \frac{3\kappa\rho H_P L}{64\sigma T^4 \pi r^2}, \tag{13}$$

where $H_P = k_B T/(\mu m_u g)$ is the pressure scale. The instability condition is then $\nabla_{\mathrm{stable}} > \nabla_{\mathrm{ad}}$.

[1] See N/A (2023) for a full description.

B. Mean molecular weight

When calculating the mean molecular weight μ, we use the mass fractions presented in Table I, and

$$\mu = \left(\sum \frac{\text{free particles}}{\text{nucleons}} \cdot \text{mass fraction}\right)^{-1}. \tag{14}$$

Inserting values yields $\mu = 0.618$.

Mass fractions

Symbol	Fraction	Element	Symbol	Fraction	Element
$\mathbf{X}$	0.7	${}^{1}_{1}\mathrm{H}$	$\mathbf{Z_{{}^{7}_{3}Li}}$	10^{-7}	${}^{7}_{3}\mathrm{Li}$
$\mathbf{Y}$	0.29	${}^{4}_{2}\mathrm{He}$	$\mathbf{Z_{{}^{7}_{4}Be}}$	10^{-7}	${}^{7}_{4}\mathrm{Be}$
$\mathbf{Y_{{}^{3}_{2}He}}$	10^{-10}	${}^{3}_{2}\mathrm{He}$	$\mathbf{Z_{{}^{14}_{7}N}}$	10^{-11}	${}^{14}_{7}\mathrm{N}$

Table I: Fractional element mass abundances assumed in this model.

C. Model

1. *Goals*

When we create this model, there are three main goals we want to reach.

1. L, M, and R should go to zero, or at least within 5% of L_0, M_0, and R_0, respectively.

2. Has a core, where $L < 0.995L_0$, reaching out to at least 10% of R_0.

3. Has a continuous convection zone ($F_{\mathrm{con}} > 0$) near the surface of the star. The width of this convection zone should be at least 15% of R_0. There can also be a convection zone closer to the stellar core, but the convective flux here should not be greater than the convective flux near the surface.

2. *Constructing the model*

Initially, we use the parameters shown in Table II. These are then scaled in order to meet the goals described in Sect. II C 1. With these values, we try to fit a model, and we do not scale any variable with more than a factor of 5, except the density.

D. Variable step length

In order to assure that no variable changes too much during the integration of Eqs. 1-4, we implement variable step length. By setting a value p, we choose the minimum

Parameter	Symbol	Value	Unit
Luminosity	L_0	1.0	$L_\odot$
Radius	R_0	1.0	$R_\odot$
Mass	M_0	1.0	$M_\odot$
Density	ρ_0	$1.42 \cdot 10^{-7}$	$\bar{\rho}_\odot$
Temperature	T_0	5770	K

Table II: Initial parameters used in the model. The quantity $\bar{\rho}_\odot$ is the average mass density of the Sun, given as $\bar{\rho}_\odot = 1.408 \cdot 10^3 \text{kgm}^{-3}$.

value of

$$\left\{ \frac{pr}{|\partial_m r|}, \frac{pP}{|\partial_m P|}, \frac{pL}{|\partial_m L|}, \frac{pT}{|\partial_m T|} \right\} \tag{15}$$

at each iteration, where ∂_m is a short-hand notation for $\partial/\partial m$. In this way, no variable changes more than p Throughout this paper, we use the value $p = 0.01$.

III. RESULTS

A. Experimenting with parameters

In order to get an idea about how the model will be affected by only changing one and one individual parameter, we run a total of 12 simulations. For the radius and temperature, we scale them up by a factor of 2, 5, and 10. For the density and pressure, the factors are 10^2, 10^3, and 10^4. Figure 1 shows the effect these scalings have on mass, radius, and luminosity as functions of radius. The parameter that has been changed can be read at the top of their respective plot. The final values for the mass and radius are shown in Table III[2] as percentages of the initial values. The luminosity is shown as the fraction of the initial luminosity. We see that the top-right and bottom-left plots are fairly identical, representing scalings to temperature and density, respectively. The changes are greater when scaling the radius and pressure, and the latter causes the model to fail entirely. This can be seen from the mass rapidly going to zero or the luminosity not changing at all. When scaling the initial radius by a factor of 5, the model represents the entire star, since $R \to 0$. When the change is only applied to the temperature or density, none of the models does so, as the radius ends up at over 5% of R_0. In the models created with varying initial pressure, we see that only one value of P_0 makes $R \to 0$, $10^2 P_0$.

[2] It is our belief that even though this table is hard to read, including it in this format is the optimal way of presenting it.

B. Final model

As the goal is not general, the only way to find the best parameters is through trial and error. We ended up with the following parameters.

$$M_0 = 0.95 M_\odot \tag{16}$$
$$R_0 = 1.6 R_\odot \tag{17}$$
$$L_0 = 0.55 L_\odot \tag{18}$$
$$\rho_0 = 1.278 \bar{\rho}_\odot \tag{19}$$
$$T_0 = 11540 \text{ K} \tag{20}$$

With these parameters, the final mass is 1.784% of M_0, and the final radius is 0.049% of R_0. For the luminosity, the final value is $1.62 \cdot 10^{-9} L_0$. The final temperature is 74.790 MK. In Figure 2, the results from the model regarding M, R, L, and T is shown. The temperature plot shows that the temperature decreases rapidly from the middle of the core and flattens out towards the surface. The mass follows a smoother curve and the luminosity reaches its maximum of around 50% of L_0 very close to the core. Both the density and pressure curves are similar in shape, with the pressure curve over ten orders of magnitude higher than that of density. The core of this model extends out to 15.29% of R_0, which is around the same value at which the mass starts to increase the most.

The fractions of energy being transported by convection and radiation (F_{con} and F_{rad}) are shown in Figure 3. As previously mentioned, if there is no convection, the convective flux equals zero. We see that there is some convection inside the core, but only radiation in the innermost part of the core. Towards the surface, there is only radiation. At the outermost part of the star, close to the surface, we find an area of convection again. This area has a width of 14.42% of R_0.

In our previous paper (N/A 2023), we presented the model used here for calculating the relative energy production from the PP branches and the CNO cycle. For the model presented in the current paper, the relative energies are shown in Figure 4. At the center of the stellar core (0,049% of R_0) the CNO cycle can be seen to have a small contribution to the total energy production (see the cut-out in Figure 4). The PP1 branch dominates in the near-surface area, where the temperature is in the range $3.385 \cdot 10^6$ K to $4.684 \cdot 10^6$ K. Here, the PP2 branch gains dominance, up to $7.121 \cdot 10^7$ K, where the PP3 branch becomes dominant. Most of the energy is being produced near the stellar core, shown as the dotted curve in Figure 4.

We present the temperature gradients in Figure 5. We see that ∇_{stable} is larger than ∇_{ad} in the region close to the core centrum, and closer to the surface, revealing that energy is being transported by convection. Close to the surface, the stable temperature gradient is more than five orders of magnitude larger than in the core. When

	$2R_0$	$5R_0$	$10R_0$	$2T_0$	$5T_0$	$10T_0$	$10^2\rho_0$	$10^3\rho_0$	$10^4\rho_0$	10^2P_0	10^3P_0	10^4P_0
$\mathbf{L_f/L_0}$	$5.2 \cdot 10^{-10}$	$2.1 \cdot 10^{-11}$	$9.4 \cdot 10^{-12}$	$7.1 \cdot 10^{-2}$	$6.9 \cdot 10^{-2}$	$5.4 \cdot 10^{-2}$	$8.6 \cdot 10^{-2}$	$8.6 \cdot 10^{-2}$	$8.6 \cdot 10^{-2}$	$1.6 \cdot 10^{-6}$	$9.9 \cdot 10^{-1}$	1.0
$\mathbf{M_f}$	3.998%	10.61%	14.50%	0.003%	0.005%	0.004%	0.013%	0.013%	0.013%	0.555%	0.008%	0.967%
$\mathbf{R_f}$	0.165%	0.336%	0.255%	6.997%	7.007%	7.048%	6.964%	6.964%	6.964%	0.014%	16.89%	75.51%

Table III: Final values f of the model after changing individual parameters. For the luminosity, the final value is shown as the fraction of the initial luminosity. The mass and radius are percentages of the initial values.

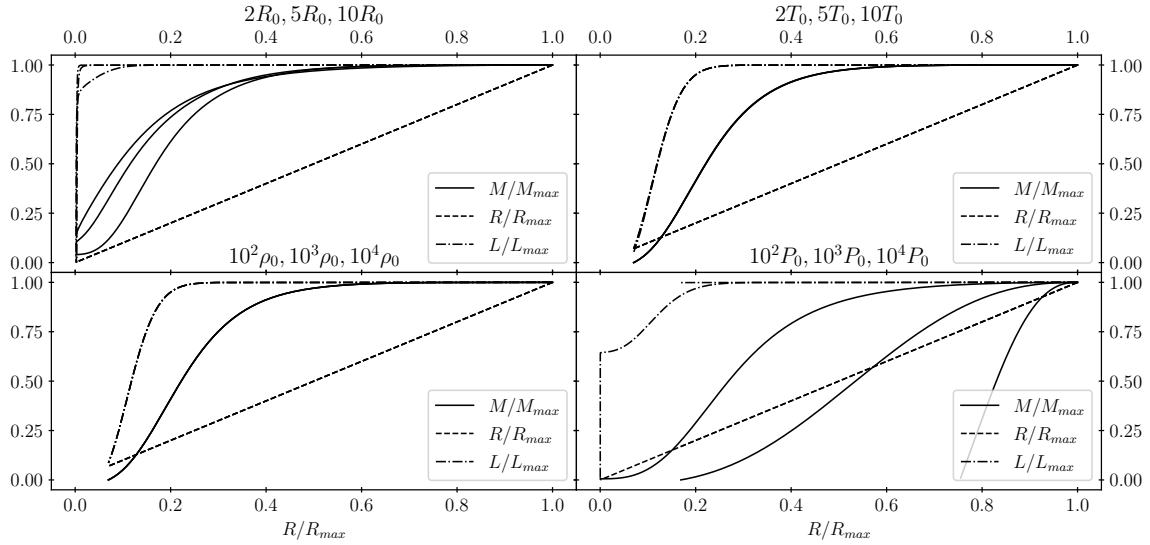

Figure 1: Mass, radius, and luminosity plotted against radius. The plots show the effect of changing individual parameters, shown above their respective plot.

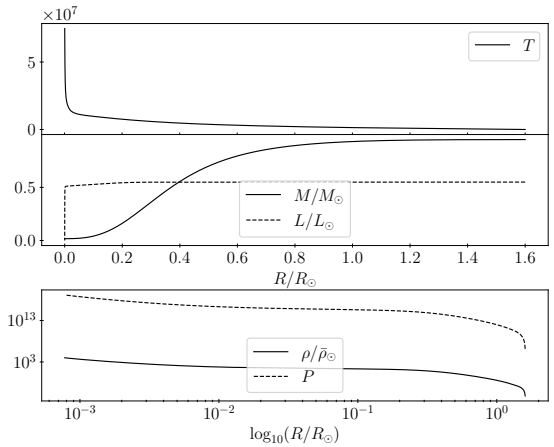

Figure 2: Temperature (top), mass and luminosity (middle), and density and pressure (bottom) in units of solar parameters, as functions of radius. The initial parameters are scaled versions of the solar parameters.

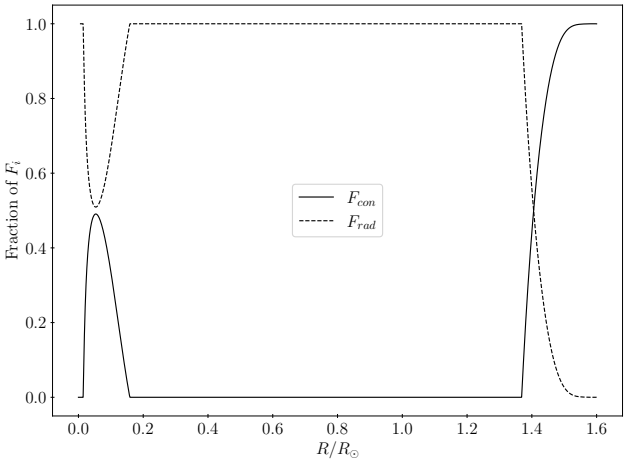

Figure 3: The fraction of energy being transported by convection (F_{con}) and radiation (F_{rad}) as functions of radius.

the radiative transfer is the transporting method, ∇^* is equal to ∇_{ad}.

Finally, we present the cross-section of the star we have modeled in Figure 6. A tiny region at the very center of the figure depicts radiation inside the stellar core. Outside of this is a convective layer, with another radiation layer outside of this. When moving out from the core, a larger layer of radiation is found. This extends out towards the surface, where the final layer of convection is

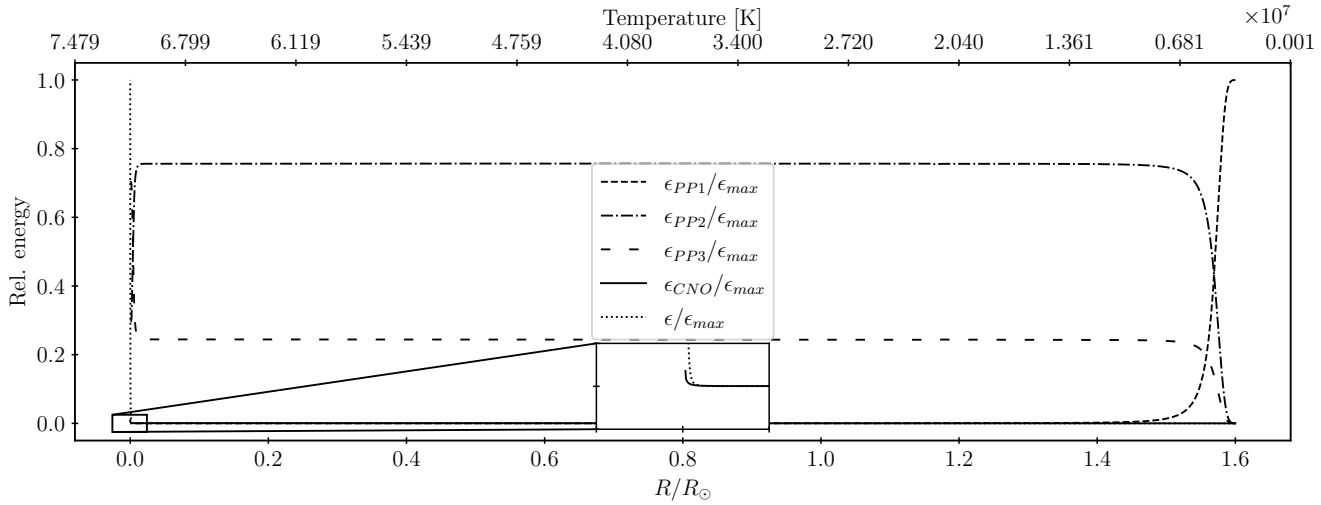

Figure 4: Relative energy production from the PP chains and the CNO cycle, as functions of radius. The corresponding temperature is also included. In the cut-out, the contribution from the CNO cycle is visible.

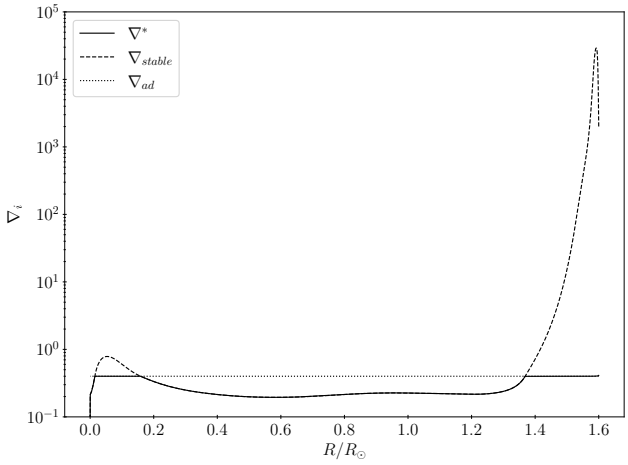

Figure 5: Temperature gradients as functions of radius. When the star is convectively stable, ∇^* is equal to ∇_{stable}. When $\nabla_{\text{stable}} > \nabla_{\text{ad}}$, energy is transported by convection.

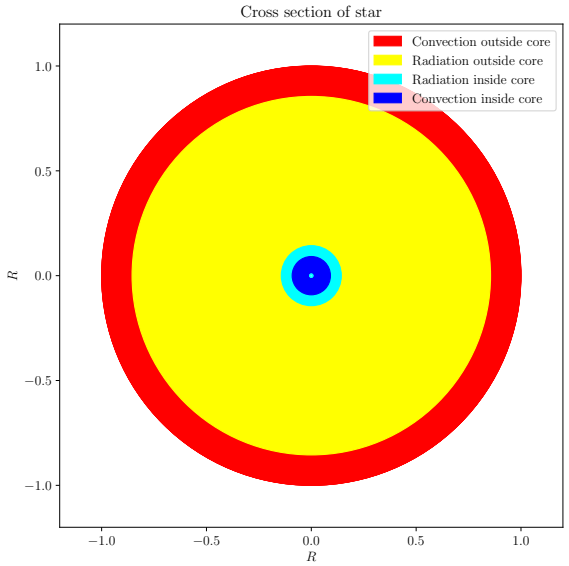

Figure 6: The cross-section of the star produced with our model. The core has a convective layer and a radiative layer. Outside of the core is another radiative layer, and another layer of convection is found closer to the stellar surface.

found.

IV. DISCUSSION

A. Finding the best parameters

As explained in Sect. III A, Figure 1 shows how the model becomes when only changing one parameter at a time. It is clear that varying the initial temperature or density does not change the results of the final model much. As the density at any step is being calculated from Eq. 8, a change in its initial value will only affect the resulting model if the initial temperature and/or pressure also changes, as $\rho = \rho(P, T)$. If there is convection (as there is at the surface), the temperature is dependent on the pressure, which again is dependent on the radius. As the model reaches the radiation layer, the dependency shifts to temperature. When the change is being done to the radius, we see that the luminosity is affected the most. As described by Eq. 3, the luminosity is only dependent on the energy output. As the

radius increases, the longer it takes before the density and temperature become large enough to affect the energy output[3]. When changing the pressure, however, the model breaks completely. Since the temperature is dependent on the pressure close to the surface, changing the pressure is affecting the model a lot.

From our testing, we do not find any indications as to which parameter needs to be changed in order to get a larger convection zone in the core. However, we find that increasing the initial radius only, results in a wider convective zone at the surface, whilst shrinking the one in the core.

B. The final model

In Sect. II C 1 we described the goals for the model. Mass, radius, and luminosity all end up well below the 5% mark, at 1.784%, 0.049%, and $1.62 \cdot 10^{-6}$%, respectively. The core luminosity is hence lower than 99.5%, reaching out to 15.29% of R_0, again satisfying the goal of at least 10%. The only goal that is not met is the width of the outermost layer of convection close to the surface. With a target width of a minimum 15% of R_0, our model fails this point, as it has a width of 14.42% of R_0. This can be caused by several things, but we assume that the increase in the initial radius while also increasing the temperature affected the resulting model.

Both Figures 3 and 5 clearly depict the core and surface convective layers. As the star has a region of radiative transfer inside the convective layer in the core, the curve for the stable temperature gradients is seen to dip towards zero as $R \to 0$ in Figure 5. When comparing to the solar cross-section in Khan *et al.* (2013), we see some similarities with regard to the different layers of our model. Mainly, we recognize the outermost convective layer with a radiative zone below. The biggest discrepancy with Khan *et al.* (2013) lies in the widths of the different layers, even though it is not stated any length measures. Our model does not have a photosphere, chromosphere, or corona either.

C. Comparison with previous work

Our previous paper (N/A 2023) aimed toward modeling the energy production from the PP branches and the CNO cycle. We found that for a star with solar density, and temperature in the range 10^4 K to 10^9 K, the PP1 branch was dominant up to $\sim 7.0 \cdot 10^4$ K, the PP2 branch up to $2.5 \cdot 10^7$ K, the PP3 branch up to $1.8 \cdot 10^8$ K, where the CNO cycle gained dominance (Figure 1 in N/A (2023)). The relative energies presented in Figure 4, show similar curves as in N/A (2023). We can barely recognize the dominant shift between the PP2 and PP3 branches before our simulation ended. Since the temperature does not reach $\sim 10^8$ K (e.g. Iliadis 2015), the region where the CNO cycle becomes the dominant energy producer is not shown. The dotted line to the left in Figure 4 shows that most of the energy is being produced inside the core.

V. CONCLUSION

In this paper, we model a star from the surface to the core. Our model is said to be sufficient if the goals presented in Sect. II C 1 are met. By running several simulations with different factors of the solar parameters, we succeed in producing a stellar model which has both a convection and radiation zone in the core, defined by where the luminosity is less than 99.5% of the surface luminosity. By implementing a variable step length to the integration, we are also able to capture large variations of the parameters with a relatively good resolution. The model reaches all of the set goals with a good margin, except for the width of the convection layer near the surface, which is a bit too narrow. When comparing to Khan *et al.* (2013), we see that our layer corresponds well with the figure they present.

As this paper is built on the model we made for calculating the energy output of a star (N/A 2023), we also compare our results for the output to the model with solar density and varying temperature. We find that the PP branches are dominant in the same regions and order we have previously found. For the CNO cycle, we can only find a marginal contribution to the total energy output in the center of the stellar core. This is also expected, as our model does not reach a high enough core temperature for the CNO cycle to reach its maximum potential.

When working on this model, we have learned a lot about how the different layers of a star have different ways of transporting the energy produced by fusion to the surface. The radiative transfer has been quite clear for the author, but how energy transport by convection works is new. Aside from this, the programming part of this project has proven itself to be the most challenging part, as usual. Numerous error messages in the terminal, combined with few, if any, mental images as to how the figures should appear, have been hard to cope with. Nevertheless, as time has gone by, and the different tasks have been solved with good assistance from fellow students and tutors, we have to say that this has been a very amusing project to work on.

[3] In (N/A 2023), the model for the energy production is dependent on temperature and density.

REFERENCES

Bethe, H. A. (1939), Phys. Rev. **55**, 434.

Gudiksen, B. V. (2022), "Ast3310: Astrophysical plasma and stellar interiors," Lecture notes.

Iliadis, C. (2015), *Nuclear physics of stars* (Wiley-VCH).

Khan, K., S. Paul, A. Zobayer, and S. Hossain (2013), International Journal of Scientific and Engineering Research **4**, 1.

N/A, (2023), "Modelling the production in stellar cores," Previous paper.

The Borexino Collaboration, (2018), Nature **562**, 505.

The British Library, (2023), "Galileo's sunspot letters," .

Appendix A: Solutions for the temperature gradients

We need to find the expression for the temperature gradients and energy flux when the plasma in the star is convectively unstable. We start with the expressions found in Gudiksen (2022), for the convective and radiative energy fluxes.

$$F_{\rm con} = \rho\, c_P T \sqrt{g\delta} H_P^{-\frac{3}{2}} \left(\frac{l_{\rm m}}{2}\right)^2 (\nabla^* - \nabla_{\rm p})^{\frac{3}{2}} \tag{A1}$$

$$F_{\rm rad} = \frac{16\sigma T^4}{3\kappa\rho H_P}\nabla^* \tag{A2}$$

$$F_{\rm rad} + F_{\rm con} = \frac{16\sigma T^4}{3\kappa\rho H_P}\nabla_{\rm stable} \tag{A3}$$

where $H_P = \frac{k_B T}{\mu m_u g}$. By inserting Eqs. A1 and A2 into Eq. A3, we find an expression for $(\nabla^* - \nabla_{\rm p})$ as a function of ∇^* and $\nabla_{\rm stable}$.

$$\frac{16\sigma T^4}{3\kappa\rho H_P}\nabla^* + \rho\, c_P T \sqrt{g\delta} H_P^{-\frac{3}{2}} \left(\frac{l_{\rm m}}{2}\right)^2 (\nabla^* - \nabla_{\rm p})^{\frac{3}{2}} = \frac{16\sigma T^4}{3\kappa\rho H_P}\nabla_{\rm stable} \tag{A4}$$

$$(\nabla^* - \nabla_{\rm p})^{\frac{3}{2}} = \underbrace{\frac{64\sigma T^3}{3\kappa\rho^2 c_P}\sqrt{\frac{H_P}{g\delta}}}_{U}\, l_{\rm m}^{-2}(\nabla_{\rm stable} - \nabla^*) \tag{A5}$$

$$\Rightarrow (\nabla^* - \nabla_{\rm p})^{\frac{3}{2}} = U l_{\rm m}^{-2}(\nabla_{\rm stable} - \nabla^*) \tag{A6}$$

The expression for the kinetic energy of the parcel is given by:

$$v = \sqrt{\frac{g\delta}{H_P}}\frac{l_{\rm m}}{2}(\nabla^* - \nabla_{\rm p})^{\frac{1}{2}} \tag{A7}$$

The gradient difference $(\nabla_{\rm p} - \nabla_{\rm ad})$ is given by:

$$(\nabla_{\rm p} - \nabla_{\rm ad}) = \frac{32\sigma T^3}{3\kappa\rho^2 c_P v}\frac{S}{Qd}(\nabla^* - \nabla_{\rm p}), \tag{A8}$$

where $S/(Qd)$ is the geometric factor. We now insert Eq. A8 into

$$(\nabla_{\rm p} - \nabla_{\rm ad}) = (\nabla^* - \nabla_{\rm ad}) - (\nabla^* - \nabla_{\rm p}), \tag{A9}$$

to obtain a second order equation for $(\nabla^* - \nabla_{\rm p})^{\frac{1}{2}}$:

$$\frac{32\sigma T^3}{3\kappa\rho^2 c_P v}\frac{S}{Qd}(\nabla^* - \nabla_{\rm p}) = (\nabla^* - \nabla_{\rm ad}) - (\nabla^* - \nabla_{\rm p}) \tag{A10}$$

$$\underbrace{\sqrt{\frac{H_P}{g\delta}}\frac{2}{l_{\rm m}}(\nabla^* - \nabla_{\rm p})^{-\frac{1}{2}}}_{v^{-1}}\frac{32\sigma T^3}{3\kappa\rho^2 c_P}\frac{S}{Qd}(\nabla^* - \nabla_{\rm p}) = (\nabla^* - \nabla_{\rm ad}) - (\nabla^* - \nabla_{\rm p}) \tag{A11}$$

$$\underbrace{\frac{64\sigma T^3}{3\kappa\rho^2 c_P}\sqrt{\frac{H_P}{g\delta}}}_{U}\frac{S}{Qd}\frac{1}{l_{\rm m}}(\nabla^* - \nabla_{\rm p})^{\frac{1}{2}} = (\nabla^* - \nabla_{\rm ad}) - (\nabla^* - \nabla_{\rm p}) \tag{A12}$$

$$\Rightarrow \frac{SU}{Qdl_{\rm m}}\xi = (\nabla^* - \nabla_{\rm ad}) - \xi^2 \tag{A13}$$

where $\xi \equiv (\nabla^* - \nabla_{\rm p})^{\frac{1}{2}}$. We further define the quantity $K \equiv SU/(Qdl_{\rm m})$.

$$\xi^2 + K\xi - (\nabla^* - \nabla_{\rm ad}) = 0 \tag{A14}$$

$$\Rightarrow \xi = \frac{-K \pm \sqrt{K^2 + 4(\nabla^* - \nabla_{\rm ad})}}{2} \tag{A15}$$

Since the pressure and temperature decrease with the radius, all of the gradients are positive. Also, the convective instability criterion ($\nabla > \nabla_{\rm ad}$) yields $\xi > 0$, resulting in

$$\xi = \frac{-K + \sqrt{K^2 + 4(\nabla^* - \nabla_{\rm ad})}}{2} \tag{A16}$$

From this, we find an expression for ∇^*:

$$\nabla^* = \xi^2 + \xi K + \nabla_{\rm ad} \tag{A17}$$

With the definition of ξ, and with the use of Eq. A17, we can rewrite Eq. A6 as follows.

$$\xi^3 = U l_{\rm m}^{-2}(\nabla_{\rm stable} - \xi^2 - \xi K - \nabla_{\rm ad}) \tag{A18}$$

$$U^{-1} l_m^2 \xi^3 + \xi^2 + K\xi + \nabla * {\rm ad} - \nabla_{\rm stable} = 0 \tag{A19}$$

By solving Eq. A19, one of the three roots will be real. This is the root we will use for the computations.